Ab initio theoretical investigation of the mechanism for α-lactone formation from α-halocarboxylates: leaving group, substituent, solvent and isotope effects

Christopher F. Rodriquez and Ian H. Williams

School of Chemistry, University of Bath, Bath, UK BA2 7AY

Structures and energetics of geometry optimized species occurring along the reaction pathway for halide elimination from α-halocarboxylates $XCHRCO_2^-$ (R = H, X = F, Cl and Br; X = Cl, R = CH_3 and $CH{=}CH_2$) have been determined by means of *ab initio* MO calculations using the HF/6-31++G(d,p) and MP2/6-311++G(d,p) methods. Endothermic heterolysis of the C_α–X bond yields halide and α-lactone by means of a transition structure leading to an ion–molecule complex lying in a shallow well. The ion–molecule complexes are all essentially planar about C_α and possess an almost completely formed C_α–O bond in the α-lactone ring. The transition structures are also essentially planar about C_α, but show only partial ring-closure. The maximum degree of charge separation occurs in the transition structure, which has considerable positive charge about C_α sandwiched between the negatively charged leaving group and internal nucleophile. Aqueous solvation, as treated by the self-consistent reaction field IPCM method, accentuates the charge-separated character of the transition structure but raises the barrier to heterolysis since the localized charge of the reactant is preferentially stabilized; the calculated value of $\Delta H^\ddagger$ = 112 kJ mol^{-1} for reaction of α-chloroacetate in water compares favourably with experimental values for hydrolyses of α-bromophenylacetic acids. Calculated secondary α-D kinetic isotope effects suggest an S_N2 transition state for reaction of α-chloroacetate but a more S_N1-like transition state for α-chloropropionate, while the α-^{14}C effects are typical of S_N2 processes. The calculated secondary β-D_3 kinetic isotope effect for α-chloropropionate is inverse.

Introduction

The observation[1] that reaction (1) of α-bromopropionate anion (**1**, R = CH_3, X = Br) in dilute sodium hydroxide occurs with retention of configuration and is independent of hydroxide ion concentration has long been regarded as a classic example of neighbouring group participation by a carboxylate group.[2] The implicated intermediate has been variously described as a zwitterion **2**,[3] an α-lactone **3**[4] or an α-lactone with much ionic character **4**.[5] Ingold considered that access of the carboxylate substituent was too limited stereochemically to allow it to form a strong bond with the carbocation centre; the intermediate therefore contained a long, weak bond of largely electrostatic character, which was nonetheless able to maintain the configuration at the α-carbon.[6] Streitwieser commented that in the absence of more definitive evidence there was little justification for not regarding the intermediate simply as an α-lactone,[7] but further experimental studies still did not resolve the issue: Kemp and Metzger[8] favoured 'an α-lactone with much ionic character', while Bordwell and Knipe preferred 'a zwitterion-like transition state where participation is electrostatic in nature, rather than an α-lactone-like transition state where participation involves covalent bond formation'.[9]

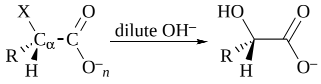

(1)

1

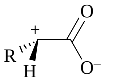

2

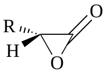

3

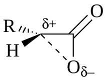

4

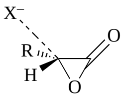

5

Shiner and McMullen attempted to resolve the controversy by measurement of secondary deuterium kinetic isotope effects (KIEs) for solvolyses of α-substituted carboxylates in water and ethanol–water solvents.[10] Their results were interpreted as being consistent with formation of a zwitterionic intermediate which could be further stabilized by a ring-closing interaction; whether or not the covalent α-lactone is formed was believed to depend on the ability of the other substituents at the α-carbon to stabilize the zwitterion and on the properties of the solvent.[11] The most recent investigation of the issue appears to be the theoretical study of Antolovic, Shiner and Davidson (ASD), which found the intermediate in the gas-phase dissociation of chloroacetate anion to be an ionic complex between the leaving group and the α-lactone (**5**, R = H, X = Cl).[11]

Our interest in the possible involvement of an α-lactone intermediate originates from on-going theoretical work in our laboratory in two areas: (*a*) strain effects upon reactivity (particularly involving three-membered rings)[12,13] and (*b*) hydrolysis mechanisms of glycosides of *N*-acetylneuraminic acid,[14] and our curiosity was aroused by a recent experimental study of the latter which suggested nucleophilic assistance by the C1 carboxylate group in the spontaneous and acid-catalysed hydrolyses of the *p*-nitrophenyl glycoside of *N*-acetylneuraminic acid, despite the formation of the strained α-lactone.[15] We now report results of *ab initio* molecular orbital (MO) calculations which extend the earlier work of ASD to consider: (*a*) the nature of the leaving group (**1**, X = F, Cl and Br), (*b*) the effect of the other α-substituent (**1**, R = H, CH_3 and $CH{=}CH_2$), (*c*) the influence of solvation, and (*d*) α-D and β-CD_3 KIEs. For each substrate, four critical points along the reaction path were examined: the α-halocarboxylate anion (comprising of the α-haloacetate, the α-chloropropionate and the α-chlorovinylacetate anions); the transition structure; the ion–molecule complex of the leaving group halide with the α-lactone; the isolated halide anion and α-lactone products.

Table 1 Calculated total energies,[a] relatve energies,[b] zero-point energies[c] and thermal energies[d]

	HF/6-31++G(d,p)				MP2/6-311++G(d,p)	
Structure	Total energy/ hartree	ΔE/kJ mol^{-1}	E_{zp}/kJ mol^{-1}	E_{th}/kJ mol^{-1}	Total energy/ hartree	ΔE/kJ mol^{-1}
1HF	−326.115 73	0	119	12	−327.179 89	0
6HF	−326.031 86	220	110	13		
5HF	−326.036 33	208	110	14		
3H	−226.576 43		110	9	−227.376 51	
F$^-$	−99.418 59			6	−99.697 59	
3H + **F**$^-$	−325.995 02	317	110	15	−327.074 10	275
1HCl	−686.165 39	0	114	13	−687.194 48	0
6HCl	−686.127 94	98	108	13	−687.152 30	111
5HCl	−686.140 01	67	111	15	−687.155 56	102
3H	−226.576 43		110	9	−227.376 51	
Cl$^-$	−459.539 66			6	−459.752 77	
3H + **Cl**$^-$	−686.116 10	129	110	15	−687.129 28	171
1HBr	−2796.591 05	0	122	13	−2800.389 64	0
6HBr	−2796.559 95	82	108	13	−2800.358 30	82
5HBr	2796.572 58	49	111	15	−2800.363 33	69
3H	−226.576 43		110	9	−227.376 51	
Br$^-$	−2569.971 27		6		−2572.962 98	
3H + **Br**$^-$	−2796.547 70	114	110	15	−2800.339 49	132
1MCl	−725.204 79	0	192	16	−726.415 25	0
6MCl	−725.169 53	93	186	18	−726.372 20	113
5MCl	−725.187 37	46	190	18	−726.381 74	88
3M + **Cl**$^-$	−725.163 47	108	188		−726.352 96	164
1VCl	−763.049 83	0	207	18		
6VCl	−763.011 99	99	200	20		
5VCl	−763.034 06	41	205	20		
3V + **Cl**$^-$	−763.008 25	109	204	20	−764.346 24	
(**1HCl**)$_s$[e]	−686.271 21	0				
(**6HCl**)$_2$[e]	−686.226 07	118				
(**5HCl**)$_s$[e]	−686.240 99	84				
(**3H**)$_s$[e]	−226.590 74					
(**Cl**$^-$)$_s$[e]	−459.651 47					
(**3H** + **Cl**$^-$)$_s$[e]	−686.242 21	76				

[a] Total energies in hartree = (1 hartree = 2625 kJ mol^{-1}). [b] Relative energies in kJ mol^{-1}. [c] Unscaled vibrational zero-point energies in kJ mol^{-1}. [d] Thermal energies in kJ mol^{-1}. [e] Single-point SCRF(IPCM)/6-31++G(d,p) energies for aqueous solvation.

Computational methods

All calculations were carried out using the GAUSSIAN92 and 94 series of programs.[16,17] Geometry optimizations were performed without any symmetry constraints at the Hartree–Fock (HF) level using the 6-31++G(d,p) basis set;[18,19] geometry optimizations including electron correlation were performed using second order Møller–Plesset correction terms[20] with the 6-311++G(d,p) basis[21] for the α-haloacetate and α-halopropionate species. Critical points on the HF potential energy surface were characterized by harmonic vibrational frequency calculations, which were also used to compute zero-point energies and thermal energies at 298 K. Intrinsic reaction coordinate calculations were used (except for the vinyl-substituted species) to verify that the respective transition structures **6** were associated with interconversion of the α-halocarboxylate anions **1** to the ion–molecule complexes **5** (Fig.1).

The effect of aqueous solvation upon the reaction energetics of (**1**, X = Cl) was determined by means of single-point self-consistent reaction field calculations using the isodensity-surface polarized continuum model (IPCM)[22] at the HF/6-31++G(d,p) level, with a relative permittivity of 78.36 and a value of 10^{-3} electron bohr^{-3} for the isodensity contour defining the shape of the molecular cavity. In this model, which is based on Onsager's reaction field theory, the solvent is considered as a uniform dielectric and the solute is assumed to occupy a cavity determined self consistently from an isodensity surface. The PCM method involves the calculation of point charges on the cavity surface which mimics the reaction field. The magnitude of these charges is proportional to the derivative of the solute electrostatic potential at each surface point. The point charges are then included in the one-electron Hamiltonian which includes polarization of the solute. This process is repeated until the surface charges are self consistently equilibrated in the solute charge distribution.

Kinetic isotope effects were evaluated from the HF geometries and cartesian force constants using the CAMVIB and CAMISO programs;[23] unwanted contamination by spurious translational and rotational contributions (which give rise to small non-zero frequencies for translational and rotational motion) were eliminated by a projection method, and the resulting pure vibrational frequencies for isotopomeric species satisfied the Teller–Redlich product rule, being entirely consistent with the masses and moments of inertia obtained from the molecular geometries.[24]

Results and discussion

Fig. 1 shows a schematic energy profile for halide elimination from the α-halocarboxylate anion **1** *via* transition structure **6** to the ion–molecule complex **5** and finally the α-lactone **3**. Total energies of all optimized structures are given in Table 1, together with vibrational zero-point and thermal energies. In the subsequent discussion structures derived from α-haloacetate anions are identified as, *e.g.* **6HBr** to denote the transition structure with R = H and X = Br, whereas structures derived from α-chloropropionate and α-chlorovinylacetate anions are identified as, *e.g.* **6MCl** (transition structure with R = CH_3, X = Cl) or **5VCl** (ion–molecule complex with R = $CH{=}CH_2$, X = Cl). Optimized values for selected geometrical parameters are given in Table 2; the atomic labelling scheme is shown for structure **1**.

Energetics of α-lactone forming halide elimination

It makes sense first to consider the gas-phase reaction energet-

Table 2 Selected HF/6-31++G(d,p) and (*in italics*) MP2/6-311++G(d,p) optimized geometrical parameters

	C_α–X/Å	C_α–O_n/Å	C–C_α/Å	C–O_n/Å	C=O_x/Å	∠CC_αX (°)	∠C_αC=O (°)	∠$C_\alpha CO_n$ (°)	ΣC_α
1HF	1.385	2.298	1.542	1.239	1.226	115.2	118.4	111.0	327.3
	1.406	*2.314*	*1.550*	*1.261*	*1.248*	*115.6*	*118.6*	*110.4*	*326.8*
6HF	2.264	1.639	1.432	1.284	1.186	123.9	149.9	74.0	360.1
5HF	2.706	1.539	1.427	1.293	1.185	130.3	154.4	68.7	358.6
3H		1.483	1.434	1.302	1.171		155.1	65.4	
		1.535	*1.450*	*1.334*	*1.191*		*154.3*	*66.8*	
1HCl	1.817	2.288	1.555	1.237	1.222	117.3	119.4	109.5	327.5
	1.802	*2.309*	*1.563*	*1.260*	*1.244*	*117.0*	*119.3*	*109.3*	*326.0*
6HCl	2.554	1.824	1.463	1.262	1.190	122.0	140.0	83.7	357.0
	2.547	*1.759*	*1.454*	*1.309*	*1.207*	*118.4*	*145.6*	*78.9*	*359.0*
5HCl	3.315	1.515	1.429	1.297	1.180	150.6	155.2	67.5	329.4
	3.113	*1.578*	*1.443*	*1.329*	*1.200*	*145.4*	*154.0*	*69.3*	*327.9*
1HBr	1.983	2.404	1.554	1.237	1.221	117.0	119.6	109,1	330.1
	1.968	*2.299*	*1.563*	*1.260*	*1.243*	*117.4*	*119.5*	*108.6*	*327.9*
6HBr	2.676	1.840	1.466	1.260	1.190	121.9	139.2	84.5	356.7
	2.649	*1.789*	*1.459*	*1.305*	*1.208*	*118.2*	*144.0*	*80.5*	*358.2*
5HBr	3.457	1.513	1.430	1.296	1.180	158.0	155.1	67.2	358.5
	3.312	*1.572*	*1.444*	*1.330*	*1.199*	*146.4*	*154.2*	*68.9*	*358.6*
1MCl	1.831	2.305	1.560	1.237	1.223	114.3	118.8	110.5	329.8
	1.808	*2.324*	*1.565*	*1.260*	*1.247*	*114.4*	*118.6*	*110.2*	*328.5*
6MCl	2.666	1.877	1.472	1.259	1.192	118.0	137.7	86.4	357.3
	2.554	*1.786*	*1.457*	*1.308*	*1.208*	*112.2*	*144.6*	*80.2*	358.4
5MCl	3.478	1.526	1.431	1.296	1.181	145.0	154.8	67.8	358.4
	3.287	*1.584*	*1.444*	*1.329*	*1.202*	*147.9*	*153.8*	*69.6*	358.7
3M		1.492	1.435	1.302	1.173		155.1	65.8	
		1.549	*1.451*	*1.336*	*1.193*		*154.1*	*67.3*	
1VCl	1.812	2.413	1.577	1.236	1.219	114.7	118.8	109.9	329.8
6VCl	2.699	1.921	1.483	1.255	1.193	116.4	135.5	88.8	356.3
5VCl	3.611	1.532	1.436	1.293	1.181	135.3	154.2	68.1	354.7
3V		1.498	1.440	1.299	1.172		154.7	66.1	
		1.569	*1.457*	*1.331*	*1.172*		*152.9*	*68.3*	

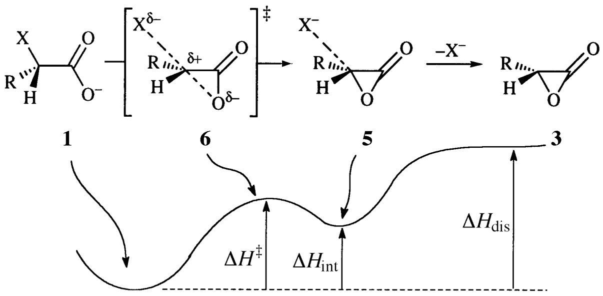

Fig. 1 Schematic energy profile for α-lactone forming halide elimination from α-halocarboxylate anion

Table 3 Calculated relative enthalpies (kJ mol^{-1}, 298 K) for structures along reaction path (Fig. 1) for α-lactone formation from α-halocarboxylate anions

	$\Delta H^‡$/kJ mol^{-1}		ΔH_{int}/kJ mol^{-1}		ΔH_{dis}/kJ mol^{-1}	
Substrate	HF	MP2	HF	MP2	HF	MP2
1HF	213	*a*	202	*a*	312	271
1HCl	94	106	67	102	124	166
1HBr	77	79	49	70	113	132
1MCl	87	108	45	87	108	163
1VCl	95	—	42	—	102	—
$(\mathbf{1HCl})_s$	112	—	83	—	74	—

[a] No stationary point on MP2 surface.

ics; the effects of aqueous solvation are discussed later. Table 3 contains calculated relative enthalpies (kJ mol^{-1}, 298 K) for structures along the reaction path (Fig. 1) for α-lactone forming elimination of halide anion from each of the substrates. The α-halocarboxylate anion **1** is the most stable species and the dissociated products, halide and α-lactone **3**, are highest in energy. The ion–molecule complex **5** between the halide anion and the α-lactone is intermediate in energy and is separated from the α-halocarboxylate by a low barrier corresponding to a transition structure **6**; however, neither of these species exists on the MP2 surface for X = F, R = H. All the energies are modified significantly by the inclusion of electron correlation at the MP2 level, but a comparison between the MP2(full) and single-point MP2(frozen-core) energies for X = Cl, R = H shows very little difference (<1.7 kJ mol^{-1}).

Measurements of appearance energies from low energy collision-induced dissociation (CID) experiments[25] yield upper limits for the gas-phase heterolytic dissociation energies ΔH_{dis} for **1HCl** and **1HBr** of 137 ± 21 and 100 ± 39 kJ mol^{-1}, respectively. By comparison, the respective MP2 calculated values of 166 and 132 kJ mol^{-1} may be a little too high; note that any basis-set superposition error would cause the dissociation energy to be overestimated. The markedly smaller dissociation energies for X = Cl and Br than for X = F reflect the greater polarizabilities of the larger halide anions.

The gas-phase dissociation energy ΔH_{dis} for **1HF** is calculated to 271 kJ mol^{-1} at the MP2 level of theory. In the CID experiments an accurate threshold measurement could not be obtained owing to the low yield of fluoride ions, but qualitatively the appearance energy for production of F^- from **1HF** was thought to be comparable with the threshold energy (246 ± 21 kJ mol^{-1}) for decarboxylation (2). An endothermicity

$$FCH_2CO_2^- \longrightarrow FCH_2^- + CO_2 \qquad (2)$$

of 262 kJ mol^{-1} for heterolytic dissociation (3) may be determined by use of the experimental enthalpies of formation for

$$FCH_2CO_2^- \longrightarrow F^- + C_2H_2O_2 \qquad (3)$$

the anions $FCH_2CO_2^-$ and F^- from the Lias compilation[26] and the *ab initio* calculated enthalpy of formation for **3H** reported in the preceding paper.[12]

Thus the calculated energies ΔH_{dis} for heterolytic dissociation

Table 4 Pauling bond orders, percentage planarities and group charges from HF/6-31++G(d,p) structures

	n(C$_\alpha$–X)	n(C$_\alpha$–O$_n$)	%planarity	q(X)	q(RC$_\alpha$H)	q(OCO$_n$)
1HF	1.0	—	−4	−0.43	+0.37	−0.94
6HF	0.23	0.77	100	−0.90	+0.48	−0.58
5HF	0.11	0.91	96	−0.91	+0.42	−0.51
3H + **F**$^-$	—	1.0	94	−1.00	+0.34	−0.34
1HCl	1.0	—	−3	−0.23	+0.10	−0.87
6HCl	0.29	0.57	91	−0.80	+0.41	−0.60
5HCl	0.08	0.95	94	−0.97	+0.34	−0.37
3H + **Cl**$^-$	—	1.0	94	−1.00	+0.34	−0.34
1HBr	1.0	—	5	−0.38	+0.17	−0.79
6HBr	0.32	0.55	90	−0.82	+0.37	−0.55
5HBr	0.09	0.95	95	−0.96	+0.38	−0.42
3H + **Br**$^-$			94	−1.00	+0.34	−0.34
1MCl	1.0	—	4	−0.27	+0.14	−0.87
6MCl	0.25	0.53	91	−0.84	+0.49	−0.66
5MCl	0.06	0.94	95	−0.95	+0.37	−0.42
3M + **Cl**$^-$	—	1.0	94	−1.00	+0.35	−0.35
1VCl	1.0	—	4	−0.14	+0.02	−0.88
6VCl	0.23	0.49	88	−0.84	+0.50	−0.66
5VCl	0.05	0.94	83	−0.92	+0.29	−0.37
3V + **Cl**$^-$	—	1.0	94	−1.00	+0.27	−0.27
(**1HCl**)$_s$				−0.20	+0.16	−0.96
(**6HCl**)$_s$				−0.88	+0.54	−0.66
(**5HCl**)$_s$				−1.01	+0.38	−0.37
(**3H** + **Cl**$^-$)$_s$	—			−1.00	+0.43	−0.43

of **1** (X = F, Cl and Br) are in fair agreement with available experimental data. Now consider what the calculated energetic results suggest concerning the existence of the ion–molecule complexes **5** in the gaseous state.

The endothermicity ΔH_{int} of the ion–molecule complex relative to the α-haloacetate anion decreases along the series **5HF**, **5HCl** and **5HBr**, in line with the dissociation energy ΔH_{dis}. Correspondingly, the barrier heights for the forward reaction diminish along this series, whereas the barriers for the reverse reaction increase, in accord with the Hammond Postulate.[27] The HF barrier heights $\Delta H^‡$ and endothermicities ΔH_{int} may be correlated by the Marcus relation[28] with an intrinsic barrier height of *ca.* 56 kJ mol^{-1}. The MP2 endothermicities are appreciably greater than the HF values, and the barriers ($\Delta H^‡ - \Delta H_{\text{int}}$) for the reverse reaction become very small (<4 kJ mol^{-1} for **5HCl**); as noted above, neither the transition structure **6HF** nor the ion–molecule complex **5HF** is a stationary point on the MP2 surface for X = F. In view of the very low barriers for collapse of **5HCl** and **5HBr** back to the α-haloacetates **1HCl** and **1HBr**, it may be that these ion–molecule complexes do not exist at ambient temperatures in the gas phase.

Replacement of a hydrogen atom by a methyl or a vinyl group on the α-carbon of the α-chlorocarboxylate stabilizes the ion–molecule complex by 22–25 kJ mol^{-1} at the HF level, with corresponding reductions in $\Delta H^‡$; at the MP2 level the stabilization is a little less. The barriers to the reverse reactions from **5MCl** and **5VCl** to **1MCl** and **1VCl**, respectively, are a little higher than for the unsubstituted ion–molecule complex **5HCl**, but even so generation of these species, and investigation of their chemistry, is likely to be difficult using current mass spectrometric techniques.

Geometries and Pauling bond orders

In view of the controversy in the literature concerning the nature of the intermediate (and/or transition state) involved in reaction (1), it is useful to consider the calculated structures for these species. Comparison of the gas-phase α-halocarboxylate anion geometries with experimental X-ray crystallographic structures is not instructive since each of the crystal structures involves interactions with a counter cation not present in the calculations, whereas the calculated structures each show incipient intramolecular interaction between the carboxylate group and C$_\alpha$.

Each transition structure has been characterized as having only one imaginary frequency. The C$_\alpha$–X distance in each transition structure **6HX** corresponds rather well with the sum of the covalent radius for carbon and the ionic radius of the halogen: 2.26, 2.55 and 2.68 Å *vs.* 2.13, 2.58 and 2.72 Å,[29] respectively, for X = F, Cl and Br. Further extension of the C$_\alpha$–X bond leads to the ion–molecule complexes **5HX**, in which a halide anion is loosely associated with the α-lactone. All of the structures with R = H possess a plane of symmetry containing the non-hydrogen atoms with the exception of the ion–molecule complex **5HF**, in which the fluoride anion is tilted out of plane towards one of the hydrogen atoms.

There are no experimental data available for bond lengths in α-lactones, but it may be useful to consider acyclic esters and δ, γ and β-lactones: the average CH$_2$–OC(O) bond length increases from 1.452 to 1.461, 1.464 and 1.492 Å along this series, while the average CO–C(O) bond length also increases from 1.336 to 1.339, 1.350 and 1.359 Å.[30] If the trend with diminishing ring size continues, bond lengths of >1.492 Å for C$_\alpha$–O$_n$ and >1.359 Å for C–O$_n$ would be expected. In this case, the C$_\alpha$–O$_n$ bond length calculated for the α-lactone **3H** may be too short at the HF level (1.483 Å), but approximately correct at the MP2 level (*ca.* 1.535 Å) and the C–O$_n$ bond length may be too short at both HF and MP2 levels (1.302 and 1.334 Å).

A useful way to interpret bond-length displacements is to express them as Pauling bond orders n according to the relation $n = \exp[(r_1 - r_n)/c]$, where r_1 and r_n are lengths for bonds of order 1 and n. Although a value of 0.3 for the constant c has been widely employed, we have noted elsewhere[31] that this value correlates changes in bond orders >1, due largely to changes in the degree of π-bonding and that a different value is more appropriate for changes in bond order <1 which are due largely to changes in the degree of σ-bonding. A value $c = 0.6$ is adopted here. Table 4 contains Pauling bond orders obtained in this manner from the HF optimized bond lengths in Table 2 for C$_\alpha$–X and C$_\alpha$–O$_n$; for this purpose the C$_\alpha$–X bond in **1** and the C$_\alpha$–O$_n$ bond in **3** are each regarded as having a bond order of unity. The ion–molecule complexes **5** show approximate conservation of bond order about C$_\alpha$ in that the sum of the bond orders for the partial bonds C$_\alpha$–X and C$_\alpha$–O$_n$ is *ca.* 1.0. Moreover, it is evident that the α-lactone ring formation is substantially complete in the ion–molecule complexes, with n(C$_\alpha$O$_n$) ⩾ 0.91. In contrast, the degree of ring closure in the transition structures **6HX** is markedly less, with n(C$_\alpha$O$_n$) decreasing along the series X = F, Cl and Br from 0.77 to 0.57 to 0.55, consistent with a less product-like transition structure for a less endothermic reaction. Similarly, variation of the C_α substituent R = H, CH_3 and CH=CH_2 in transition structures **6RCl** leads to a decrease in $n(C_\alpha O_n)$ from 0.57 to 0.53 to 0.49; also the sum of the bond orders for C_α–X and C_α–O_n decreases along this series, suggesting a looser transition structure.

Heterolytic cleavage of the C_α–X bond is accompanied by a change of geometry about C_α from tetrahedral towards trigonal planar, and intramolecular nucleophilic attack by O_n involves further change towards the inverted tetrahedral arrangement about C_α. A measure of this structural alteration along the reaction coordinate is provided by the fractional change in the sum (ΣC_α) of the three angles $CC_\alpha R$, $CC_\alpha H$ and $RC_\alpha H$ between 328.4° (=3 × tetrahedral angle, 109.47°) and 360°, expressed as a percentage. These values, given in Table 4, show that the ion–molecule complexes are all essentially planar about C_α, despite the almost complete formation of the C_α–O_n bond in the α-lactone ring. Moreover, each of the transition structures and each of the α-lactone products is also essentially planar about C_α.

Table 5 Calculated kinetic isotope effects (298 K) for α-lactone formation from α-halocarboxylate anions

	HF	**HCl**	**HBr**	**MCl**	**VCl**
$k_{\mathbf{H}}/k_{\alpha\text{-D}}$	1.033	1.020	1.013	1.099	1.059
MMI	1.0159	1.0105	1.0097	1.0047	1.0051
EXC	1.0013	1.0019	1.9995	0.9739	0.9733
ZPE	1.0155	1.0067	1.0024	1.1224	1.0821
TUN	1.0002	1.0008	1.0009	1.0007	1.0004
$k_{^{12}\text{C}}/k_{\alpha\text{-}^{14}\text{C}}$	1.111	1.121	1.114	1.093	1.075
MMI	1.0097	1.0038	1.0019	1.0002	1.0007
EXC	0.9743	0.9962	1.0008	0.9920	0.9870
ZPE	1.1275	1.1027	1.0917	1.0930	1.0830
TUN	1.0016	1.0170	1.0174	1.0090	1.0045
$k_{\mathbf{H}}/k_{\beta\text{-D}_3}$				0.966	
MMI				1.0144	
EXC				0.9063	
ZPE				1.0484	
TUN				1.0026	

Charges

Another important aspect concerning the structures of intermediate **5** and transition state **6** is their charge distributions. Table 4 contains group charges *q* for the X, $RC_\alpha H$ and OCO_n groups, obtained by summation of Mulliken atomic charges from Hartree–Fock calculations. As expected, progress along the reaction coordinate from $\mathbf{1} \longrightarrow \mathbf{6} \longrightarrow \mathbf{5} \longrightarrow \mathbf{3}$ is accompanied by increased negative charge on the halide and decreased negative charge on the carboxylate moiety. The $RC_\alpha H$ group appears to be positively charged throughout, generally with a larger charge in the α-lactone than in the α-halocarboxylate. The point of interest, however, is that in each case the maximum positive charge on the $RC_\alpha H$ group is found in the transition structure rather than in the ion–molecule complex; indeed the maximum degree of charge separation occurs in the transition structure for α-lactone formation.

The charge on the $RC_\alpha H$ group in each ion–molecule complex is almost the same as in the α-lactone, except that in **5HF**: the asymmetric character of this species, as noted above, with some interaction between the fluorine atom and one of the hydrogens, distinguishes it from the other ion–molecule complexes.

Solvation

Since all the experimental investigations of reaction (1) are in solution, it is essential to consider the effects of solvation upon the calculated properties discussed above. Single-point SCRF(IPCM)/6-31++G total energies for species along the reaction path for α-lactone forming elimination of chloride from α-chloroacetate anion $(\mathbf{1HCl})_s$ in water are given in Table 1, and relative enthalpies are presented in Table 3. [All attempts to perform geometry optimizations with the SCRF(IPCM) method failed to yield converged wavefunctions.] The heterolytic dissociation energy ΔH_{dis} is reduced by 50 kJ mol^{-1} in aqueous solution as compared with the gas phase, owing to more favourable solvation of the localized negative charge in the free chloride anion than of the delocalized negative charge in the α-chloroacetate anion. The enthalpy of activation $\Delta H^\ddagger$ is 18 kJ mol^{-1} higher in water than in the gaseous state, consistent with a more diffuse distribution of charges within the transition structure $(\mathbf{6HCl})_s$ than the reactant $(\mathbf{1HCl})_s$; although (as noted above) the transition structure involves a greater degree of charge separation, the charge distribution is less concentrated within the volume of the molecular cavity with the polarizable continuum model for solvation. The calculated value of $\Delta H^\ddagger = 112$ kJ mol^{-1} for reaction of α-chloroacetate in water is similar to the range of values 107–125 measured by Bordwell and Knipe[9] for hydrolysis of α-bromophenylacetic acids in aqueous sodium hydrogencarbonate at 25 °C. Because the two substrates here are different, direct comparison is invalid, but nonetheless the broad similarity of the calculated and experimental values does suggest that the theoretical treatment of solvation is not unreasonable. The energy ΔH_{int} of the ion–molecule complex $(\mathbf{5HCl})_s$ relative to $(\mathbf{1HCl})_s$ is also raised by 16 kJ mol^{-1} in aqueous solution as compared with the gas phase, for a similar reason.

The effect of aqueous solvation upon the charge distribution in $(\mathbf{1HCl})_s$ as compared with **1HCl** is to increase the negative charge on the carboxylate group, but the charge distributions in the solvated and unsolvated ion–molecule complexes $(\mathbf{5HCl})_s$ and **5HCl** are almost the same. The largest change in charge distribution due to aqueous solvation, however, is experienced by the transition structure **6HCl**: the negative charges *q*(Cl) and $q(OCO_n)$ on the chloride and carboxylate moieties in $(\mathbf{6HCl})_s$ are more negative, and the positive charge $q(RC_\alpha H)$ on the substituted C_α moiety is more positive.

Kinetic isotope effects

Table 5 contains α-D and α-^{14}C kinetic isotope effects calculated for α-lactone formation from each α-halocarboxylate anion (and the β-D_3 KIE for the α-chloropropionate system) at 298 K, together with the mass-moment-of-inertia (MMI), excitational (EXC) and zero-point-energy (ZPE) factors of the semi-classical isotope effect[32] and the tunnelling (TUN) factor evaluated using the Bell equation.[33]

The magnitude of an α-D KIE for nucleophilic substitution depends upon the nature of the nucleophile, leaving group, α-substituent and solvent, but generally serves to discriminate between S_N2-like and S_N1-like mechanisms of reaction: the former typically show values close to unity (either normal or inverse) while the latter usually display much larger normal values. In either case, the magnitude of the effect would be expected to depend upon the leaving group in the order F > Cl > Br, the order of the deuterium fractionation factors[34] which reflect the decreasing stiffness of bonding in the reactant. The calculated α-D KIEs for the fluoro-, chloro- and bromoacetates are indeed in this order.

The low value of $k_{\mathbf{H}}/k_{\alpha\text{-D}} = 1.02$ for the unsubstituted chloroacetate **HCl** (Table 5) is characteristic of an S_N2 mechanism. A methyl substituent at C_α increases KIE for the **MCl** reaction to a value of 1.10 suggestive of a much more S_N1-like transition state; the accepted maximum value[35] of $k_{\mathbf{H}}/k_{\alpha\text{-D}}$ for limiting reactions involving no covalent attachment of a chloride leaving group (or of a solvent nucleophile) is *ca.* 1.15. Vinyl substitution at C_α, as in **VCl**, increases the isotope effect by a lesser amount to 1.06. Although the bond orders $n(C_\alpha\text{–Cl})$ and $n(C_\alpha\text{–}O_n)$ are smaller for the transition structure **6VCl** than for **6MCl** (which would suggest a looser, more S_N1-like transition state), the normal contribution to KIE arising from the bending motions about C_α, is significantly offset by an inverse factor due to the C_α–H stretching mode.[36] The C_α–H stretching force constants in **6VCl** (6.67 mdyn Å^{-1}), **6MCl** (6.66 mdyn Å^{-1}) and **6HCl** (6.69 mdyn Å^{-1}) are all very similar but that in **1VCl** (5.87 mdyn Å^{-1}) is significantly lower than in either **1MCl** or **1HCl** (5.99 mdyn Å^{-1}). This suggests there is some hyperconjugation between the C_α–H bond and the vinyl substituent in **1VCl** which is lost in the transition structure **6VCl**, giving rise to a larger inverse contribution to the KIE than for the propionate or acetate species.

The magnitudes of α-^{14}C KIEs are generally substantially lower in S_N1 than in S_N2 reactions, which are usually in the range 1.06–1.15 at room temperature. All the HF/6-31++G(d,p) calculated results (Table 5) fall within this range. The semi-classical KIEs for **HF**, **HCl** and **HBr** depend upon the leaving group in the order F > Cl > Br, as expected from the ^{14}C fractionation factors[34] which reflect the decreasing stiffness of bonding in the reactant. The tunnelling corrections for **HCl** and **HBr** are, however, surprisingly large (*ca.* 1.017) and in consequence the overall ^{14}C KIEs do not show the same trend. These relatively large tunelling contributions arise because the (imaginary) reaction-coordinate vibrational frequencies in **6HCl** and **6HBr** are particularly sensitive to isotopic substitution at C_α; the isotopic frequency shifts upon ^{14}C substitution are $-20i$ cm^{-1} as compared with only $-5i$ cm^{-1} for **6HF** and with isotopic shifts upon deuteriation of **6HF**, **6HCl** and **6HBr** of only $-1i$ cm^{-1}. The reason for this isotropic sensitivity is that for **6HCl** and **6HBr** the reaction-coordinate vibrational mode is dominated by motion of the C_α atom to a much greater extent than for any of the other transition structures. The sum of squares of the mass-weighted cartesian components is 0.64 and 0.68, respectively, as compared with only 0.30 for **6HF**. In turn this difference reflects the looser nature of **6HCl** and **6HBr** as compared with **6HF**: the sum of the bond orders $n(C_\alpha–X) + n(C_\alpha–O_n)$ is 0.86 and 0.87, respectively, as compared with 1.00 (Table 4).

The α-^{14}C KIE decreases in value along the series **HCl**, **MCl** and **VCl**. The conventional interpretation of this is that the transition structures become less S_N2-like, more S_N1-like, as the substituent on C_α stabilizes the developing carbocationic centre by means of strengthened resonance interactions. The sum of the transition-state bond orders $n(C_\alpha–X) + n(C_\alpha–O_n)$ decreases from 0.86 to 0.78 and 0.72 along this series, indicating increasingly loose transition structures. Comparison of the C_α–C_β bond lengths and stretching force constants in **6MCl** and **6VCl**, respectively, shows a shortening (1.498–1.464 Å) and a stiffening (5.32–5.80 mdyn Å^{-1}), in accord with this interpretation, as the hyperconjugating methyl substitient is replaced by the more effective conjugating vinyl substituent. The magnitude of the tunnelling correction also diminishes along this series as the result of the decreasing value of the (imaginary) reaction-coordinate vibrational frequency.

The β-deuterium KIE (Table 5) is predicted to be inverse, with $k_H/k_{\beta\text{-}D_3} = 0.966$ for **MCl**. Although inverse β-deuterium KIEs are known in situations where the usual hyperconjugative mechanism is inoperative,[37,38] it would be expected that deuterium substitution in the methyl group of α-chloropropionate would lead to a normal KIE as the result of hyperconjugative stabilization of the developing carbocationic centre at C_α.[32] The calculated ZPE factor is indeed normal (1.048) but inspection of the C_β–H(D) stretching frequencies shows them to be greater in the transition structure than in the reactant: the average C_β–H stretching force constant is 5.76 mdyn Å^{-1} in **1MCl** and 5.91 mdyn Å^{-1} in **6MCl**. The present calculations apparently reveal no evidence for transition-state hyperconjugation between the methyl group and C_α. On the other hand, the EXC factor is considerably inverse (0.906) as the result of the loss in **6MCl** of the very low vibrational frequency (27 cm^{-1}) associated with the C_α–CO_2^- torsion in **1MCl**. This mode, which is insensitive to β-D_3 substitution in the reactant, is entropy rich; the corresponding mode in the transition state has a much higher frequency (146 cm^{-1}). The lowest-frequency mode of the transition structure involves the C_α–CH_3 torsion, with values of 73 cm^{-1} in [$^1H_3$]**6MCl** and 56 cm^{-1} in [$^2H_3$]**6MCl** as compared with >220 cm^{-1} in **1MCl**; progress from reactant to transition state is accompanied by a greater loss of vibrational entropy for protiated than for deuteriated **MCl**, thus gives rise to an inverse EXC factor. However, it should be recognized that use of the harmonic oscillator approximation in partition-function and isotope-effect calculations involving such frequencies must be considered with some suspicion.

Mechanistic implications

The controversy surrounding the detailed course of α-lactone-forming halide elimination from α-halocarboxylates has two aspects: one concerns the nature of the intermediate, the other the nature of the rate-limiting transition state. The results of the present calculations leave little room for doubt that the intermediate is best described as an α-lactone. In aqueous solution the products (halide anion + α-lactone) of heterolytic dissociation are lower in energy than the ion–molecule complex, whereas in the gaseous phase the latter is preferred enthalpically. However, all the calculations indicate that the α-lactone moiety has similar properties in both the ion–molecule complex and the dissociated products.

The present calculations for the transition structure suggest a species which possesses an approximately half-formed α-lactone ring, an essentially planar C_α, and significant ionic character with substantial positive charge on the $RC_\alpha H$ moiety sandwiched between the negative charges of the leaving group and internal nucleophile. Kemp and Metzger's description of 'an α-lactone with much ionic character'[8] therefore seems a reasonable description of the transition structure. Bordwell and Knipe referred specifically to the transition state, which they described as 'zwitterion-like . . . where participation is electrostatic in nature, rather than . . . where participation involves covalent bond formation';[9] in contrast, our results indicate substantial charge separation in a structure involving a significant degree of covalent bond formation.

Hydrolysis of the *p*-nitrophenyl glycoside of *N*-acetylneuraminic acid at pH 6.67 was found to give a lower β-D KIE than at pH 1.0 or pH 2.69; this was interpreted as evidence that the p-type orbital at C_α was much less electron-deficient when the carboxylate group was ionized and thus able to participate nucleophilically in an α-lactone-like transition state.[15] Hydrolysis of 2-*p*-tolylsulfonatopropionate in 0.05 M sodium hydroxide solution at 25 °C shows[10] $k_H/k_{\alpha\text{-}D}$ of 1.181, as compared with the maximum expected secondary α-D KIE of 1.23 for a sulfonate leaving group and $k_H/k_{\beta\text{-}D_3} = 1.074$, as compared with the maximum secondary β-D_3 KIE of 1.46 for trifluoroacetolysis of 2-propyl toluene-*p*-sulfonate. The α-D KIE is large but not maximal, and the β-D_3 KIE is small (although not inverse!): McMullen interpreted these results as indicating nucleophilic interaction between C_α and the carboxylate group.[10] On the other hand, values of $k_H/k_{\alpha\text{-}D}$ in the range 1.095–1.122 for solvolysis of 2-bromophenyl acetate in ethanol–water mixtures at 25 °C could be reconciled with the unusually low Grunwald–Winstein *m*-value only if the carboxylate group were considered to provide local ionizing power but not to interact nucleophilically with C_α in the rate-determining step.[10] McMullen described formation of 'an ion pair intermediate stabilized by orbital overlap between carboxylate oxygen and the α-carbon, which is variably partitioned between separation, return and closure to an α-lactone depending on solvent polarity and hydrogen bonding ability.'[10] These conclusions from earlier experimental work are not incompatible with the present theoretical results, but it must be admitted that the treatment of solvation employed in the present study (a continuum model without geometry optimization) is inadequate to reproduce the range of subtle possibilities envisaged by McMullen[10] or Shiner.[11] To do so would require the ability to model specific interactions with explicit solvent molecules, perhaps by means of a hybrid quantum-mechanical/molecular-mechanical method.[39,40]

Acknowledgements

We are grateful to the EPSRC for support of this work through research grant GR/J53218.

References

1 W. A. Cowdrey, E. D. Hughes and C. K. Ingold, *J. Chem. Soc.*, 1937, 1208.
2 B. Capon, *Quart. Rev.* (*London*), 1964, **18**, 75.
3 W. A. Cowdrey, E. D. Hughes, C. K. Ingold, S. Masterman and A. D. Scott, *J. Chem. Soc.*, 1937, 1252.
4 L. P. Hammett, *Physical Organic Chemistry*, McGraw-Hill, New York, 1940.
5 E. Grunwald and S. Winstein, *J. Am. Chem. Soc.*, 1948, **70**, 841.
6 C. K. Ingold, *Structure and Mechanism in Organic Chemistry*, Cornell University Press, Ithaca, 2nd edn., 1969, pp. 523–524.
7 A. Streitwieser, *Chem. Rev.*, 1956, **56**, 573.
8 K. C. Kemp and D. Metzger, *J. Org. Chem.*, 1968, **33**, 4165.
9 F. G. Bordwell and A. C. Knipe, *J. Org. Chem.*, 1970, **35**, 2956.
10 D. F. McMullen, *Doctoral Dissertation*, Indiana University, 1982.
11 D. Antolovic, V. J. Shiner and E. R. Davidson, *J. Am. Chem. Soc.*, 1988, **110**, 1375.
12 C. F. Rodriquez and I. H. Williams, *J. Chem. Soc.*, *Perkin Trans. 2*, 1997, preceding paper.
13 D. Buttar and I. H. Williams, to be submitted to *J. Chem. Soc.*, *Perkin Trans. 2*.
14 J. A. Barnes, *Ph.D. thesis*, University of Bath, 1994.
15 M. Ashwell, X. Guo and M. L. Sinnott, *J. Am. Chem. Soc.*, 1992, **114**, 10 158.
16 M. J. Frisch, G. W. Trucks, M. Head-Gordon, P. M. W. Gill, M. W. Wong, J. B. Foresman, B. G. Johnson, H. B. Schlegel, M. A. Robb, E. S. Replogle, R. Gomperts, J. L. Andres, K. Raghavachari, J. S. Binkley, C. Gonzalez, R. L. Martin, D. J. Fox, D. J. Defrees, J. Baker, J. J. P. Stewart and J. A. Pople, GAUSSIAN92, Revision C.4, Gaussian, Inc. Pittsburgh, PA., 1992.
17 M. J. Frisch, G. W. Trucks, H. B. Schlegel, P. M. W. Gill, B. G. Johnson, M. A. Robb, J. R. Cheeseman, T. Keith, G. A. Petersson, J. A. Montgomery, K. Raghavachari, M. A. Al-Laham, V. G. Zakrzewski, J. V. Ortiz, J. B. Foresman, C. Y. Peng, P. Y. Ayala, W. Chen, M. W. Wong, J. L. Andres, E. S. Replogle, R. Gomperts, R. L. Martin, D. J. Fox, J. S. Binkley, D. J. Defrees, J. Baker, J. J. P. Stewart, M. Head-Gordon, C. Gonzalez and J. A. Pople, GAUSSIAN94, Revision B.3, Gaussian, Inc., Pittsburgh, PA, 1995.
18 (*a*) R. Ditchfield, W. J. Hehre and J. A. Pople, *J. Chem. Phys.*, 1971, **54**, 724; (*b*) W. J. Hehre, R. Ditchfield and J. A. Pople, *J. Chem. Phys.*, 1972, **56**, 2257; (*c*) P. C. Hariharan and J. A. Pople, *Mol. Phys.*, 1974, **27**, 209; (*d*) M. S. Gordon, *Chem. Phys. Lett.*, 1980, **76**, 163; (*e*) P. C. Hariharan and J. A. Pople, *Theor. Chim. Acta*, 1973, **28**, 213.
19 (*a*) T. Clark, J. Chandrasekhar, G. W. Spitznagel and P. v. R. Schleyer, *J. Comput. Chem.*, 1983, **4**, 294; (*b*) M. J. Frisch, J. A. Pople and J. S. Binkley, *J. Chem. Phys.*, 1984, **80**, 3625.
20 C. Møller and M. S. Plesset, *Phys. Rev.*, 1934, **46**, 618.
21 (*a*) A. D. McLean and G. S. Chandler, *J. Chem. Phys.*, 1980, **72**, 5639; (*b*) R. Krishnan, J. S. Binkley, R. Seeger and J. A. Pople, *J. Chem. Phys.*, 1980, **72**, 650; (*c*) A. J. H. Watchers, *J. Chem. Phys.*, 1970, **52**, 1033; (*d*) P. J. Hay, *J. Chem. Phys.*, 1977, **66**, 4377; (*e*) K. Raghavachari and G. W. Trucks, *J. Chem. Phys.*, 1989, **91**, 1062.
22 T. A. Keith, J. B. Foresman and M. J. Frisch, unpublished work cited in M. J. Frisch, A. E. Frisch and J. B. Foresman, *Gaussian 94 User's Reference*, Gaussian, Inc., Pittsburgh, PA, 1995.
23 I. H. Williams, *Chem. Phys. Lett.*, 1982, **88**, 462.
24 I. H. Williams, *J. Mol. Struct.*, *THEOCHEM*, 1983, **94**, 275.
25 S. T. Graul and R. R. Squires, *Int. J. Mass Spectrom. Ion Processes*, 1990, **100**, 785.
26 S. G. Lias, J. E. Bartness, J. F. Liebman, R. D. Levin and W. G. Mallard, *J. Phys. Chem. Ref. Data*, *Suppl. 1*, 1988.
27 G. S. Hammond, *J. Am. Chem. Soc.*, 1955, **77**, 334.
28 T. H. Lowry and K. S. Richardson, *Mechanism and Theory in Organic Chemistry*, Harper and Row, New York, 3rd. edn., 1987.
29 P. Atkins, *Physical Chemistry*, Oxford University Press, Oxford, 1978.
30 *CRC Handbook of Chemistry and Physics*, eds. D. R. Lide and H. P. R. Frederikse, CRC Press, Boca Raton, FL, 77th edn., 1996.
31 J. Wilkie and I. H. Williams, *J. Chem. Soc.*, *Perkin Trans. 2*, 1995, 1559.
32 L. Melander and W. H. Saunders, *Reaction Rates of Isotopic Molecules*, Wiley, New York, 1980.
33 R. P. Bell, *The Tunnel Effect in Chemistry*, Chapman and Hall, London, 1980.
34 S. R. Hartshorn and V. J. Shiner, *J. Am. Chem. Soc.*, 1972, **94**, 9002.
35 V. J. Shiner and W. Dowd, *J. Am. Chem. Soc.*, 1971, **93**, 1029.
36 J. A. Barnes and I. H. Williams, *J. Chem. Soc.*, *Chem. Commun.*, 1993, 1286.
37 V. J. Shiner and J. S. Humphrey, *J. Am. Chem. Soc.*, 1963, **85**, 2416.
38 M. Tarle, S. Borcic and D. E. Sunko, *J. Org. Chem.*, 1975, **40**, 2949.
39 J. A. Barnes and I. H. Williams, *J. Chem. Soc.*, *Chem. Commun.*, 1996, 193.
40 J. Gao, in *Rev. Comput. Chem.*, vol. 7, eds. K. B. Lipkowitz and D. B. Boyd, VCH, New York, 1995, p. 119.

Paper 6/06819G
Received 4*th November* 1996
Accepted 20*th January* 1997